

Computationally efficient calculation of edge diffraction in time domain

Petros Nikolaou

Department of Mechanical and Aeronautical Engineering University of Patras, Patras, Greece.

Penelope Menounou

Department of Mechanical and Aeronautical Engineering University of Patras, Patras, Greece.

Summary

The fast and accurate calculation of the diffracted signal caused by edges is important in many practical cases such as road traffic noise diffracted by noise barriers. The authors presented in the past an impulse response solution for diffraction by edges. The diffracted signal is obtained by convolving the impulse response function with any given incident signal. In numerical calculations the impulse response requires fine time sampling to describe its starting values, where it becomes infinite. As a result, the computational time required, to produce convergent/accurate predictions, increases dramatically, particularly in cases involving multiple receivers. In the present work two methods are presented that reduce the computational time. The first is based on the generator curve, a curve that embodies/generates all impulse response functions produced for any source/receiver configuration, thus allowing faster impulse response calculations. The second method relies on the partial time antiderivatives of the impulse response, which are proven to be continuous non-singular functions, expressed in close form, which can replace the impulse response in predicting the diffracted signal. Compared to the impulse response the antiderivatives can produce convergent results with much lesser time samples, thus achieving significant computational advantage. Finally, generator curves are derived for the antiderivatives as well, improving their performance even further.

PACS no. 43.20El, 43.50Gf

1. Introduction

Edge diffraction is important to many areas of acoustics ranging from traffic noise barriers [1] and urban noise [2], to room acoustics [3]. The problem of diffraction by the edge of a half-plane has been extensively studied in both frequency and time domain [1]. In the time domain the solutions span from analytical solutions, both rigorous [4] and approximate [5], to experimental investigation [6] and numerical simulations [7].

In the present study we employ an analytical time domain solution [8], whose unique

characteristics/properties allow a significant reduction in the computational cost of predicting the diffracted signal around a noise barrier modeled as an infinitely thin half plane.

The typical geometry of a half plane diffraction problem is shown in Figure 1.

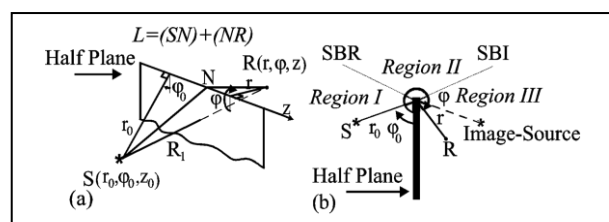


Figure 1. Geometry of the half plane diffraction problem; perspective view (a), side view (b).

The positions of the source $S(r_0, \phi_0, z_0)$ and the receiver $R(r, \phi, z)$ are given with cylindrical

coordinates. The radial distance r is measured from the edge of the half-plane and the angle ϕ is measured from the surface of the half-plane facing the source. The shortest distance that the sound travels to reach the receiver by diffraction is L . The direct distance between the source and the receiver is denoted by R_1 , while the distance from the image source to the receiver by R_2 .

According to geometrical acoustics, region III (see Figure 1b) is a shadow zone, region II includes only the incident signal, and in region I both the incident and the reflected (from the surface of the half plane) signals are present. The diffracted signal is present in all three regions. The present work focuses on this latter contribution, the diffracted signal around the half plane and specifically on methods to reduce the cost of its computation.

1.1. Analytical impulse response solution

The authors have presented an analytical impulse response solution p_{irf}^d [8] which, unlike other time domain models has a unified form for every type of incident radiation i.e. for plane, spherically and, cylindrically spreading incident signals. In the present work, results are presented for spherical incident signals and the reader is referred to ref. [8] for appropriate changes in the solution parameters that make the solution applicable to plane and cylindrically spreading incident signals, as well as to diffraction by wedges.

The impulse response derived in ref. [8] will be used in the present work as a function of *diffraction time* τ - i.e the retarded time that starts the moment the diffracted signal arrives at the receiver $\tau = t - t_d$, where for spherical incident signal the arrival time t_d becomes

$$t_d = L/c, \quad (1)$$

where c is the speed of sound.

Specifically, the impulse response solution is

$$p_{irf}^d = -\frac{1}{4\pi} A_t \cdot (I \cdot d) \quad (2)$$

$$I = \frac{2}{\sqrt{\tau(\tau + 2t_d)}} H(\tau) \quad (3)$$

$$d = d^i + d^r = \frac{\bar{t}_1 \Phi_1 \sqrt{\frac{\tau}{t_d} + 2}}{\tau + \tau_{lag}^i} + \frac{\bar{t}_2 \Phi_2 \sqrt{\frac{\tau}{t_d} + 2}}{\tau + \tau_{lag}^r} \quad (4)$$

$$p_{irf}^d = p_{irf}^{di} + p_{irf}^{dr} = -\frac{1}{4\pi} A_t \cdot (I \cdot d^i) - \frac{1}{4\pi} A_t \cdot (I \cdot d^r), \quad (5)$$

where the first terms in equations 4, 5, d^i , p_{irf}^{di} , and the parameters \bar{t}_1, Φ_1 are associated with the incident signal, while the terms, d^r , p_{irf}^{dr} , and the parameters \bar{t}_2, Φ_2 are associated with the signal reflected from the surface of the half plane. The factor I is proportional to the Green's function solution of the 2D wave equation representing radiation from a line source, where $H(\tau)$ is the Heaviside or unit step function. The function d describes the directionality of the line source, while the product $(I \cdot d)$ represents radiation from a directional line source. The factor A_t depends on the type of the incident signal,

$$A_t = \frac{1}{\sqrt{rr_0}}. \quad (6)$$

The parameters \bar{t}_1 and \bar{t}_2 have units of time and depend on various geometrical distances of the problem. For spherical incident signal become

$$\bar{t}_{1,2} = \frac{rr_0\pi}{c(L + R_{1,2})}. \quad (7)$$

The angle parameters Φ_1 and Φ_2 are functions of the angular positions of source and receiver,

$$\Phi_{1,2} = \frac{2\sqrt{2}}{\pi} \cos\left(\frac{\phi \mp \phi_0}{2}\right). \quad (8)$$

Finally, the quantities τ_{lag}^i and τ_{lag}^r are given by,

$$\tau_{lag}^{i,r} = 0.5\pi\bar{t}_{1,2}\Phi_{1,2}^2, \quad (9)$$

are termed *diffraction delay times*, and represent the time delay of the arrival of the diffracted signal compared to the arrival of the free field signal and the reflected signal, respectively.

The solution (equations 2-5) is exact for plane incident signals, while approximate for cylindrical and spherical incident signals being valid for $L/cT_{inc} > 1$ —where T_{inc} is the duration of the incident signal (i.e., invalid when both source and receiver are within one spatial extent of the incident signal, cT_{inc} , from the edge).

1.2. Digital convolution

The diffracted pulse p^d , produced when an arbitrary incident signal f reaches the edge of the half plane, is calculated as the result of the convolution of p_{irf}^d with f ,

$$p^d = p^{di} + p^{dr} = p_{irf}^{di} * f + p_{irf}^{dr} * f, \quad (10)$$

where $p_{irf}^{di} * f$ is associated with the incident signal and $p_{irf}^{dr} * f$, with the reflected signal.

A first observation for the convolution in equation 10 comes from the mathematical form of the impulse response p_{irf}^d , which goes to infinity as $\tau \rightarrow 0$. Thus, in numerical calculations a finer time sampling is required at the front of the diffracted signal in order to accurately predict the slope of the impulse response at its starting times. The computational time is then increased, especially for cases where the calculation of p_{irf}^d is performed for multiple receivers. To increase the speed of the numerical evaluation of p_{irf}^d a characteristic property of p_{irf}^d will be used. Specifically, the generator curve method detailed in section 2

In numerical computations the incident signal is sampled with a time step $d\tau$ on M time samples (f_m), while p_{irf}^{di} is discretized with the same $d\tau$ on J time samples (p_{irf}^{di}) _{j} with $J > M$ for finite incident signals (the impulse response has a larger duration than T_{inc} to describe the ending/tail of the diffracted signal) and $J = M$ for infinite incident signals. The k -th element of the digital convolution ($p_{irf}^{di} * f$) _{k} is given by the summation,

$$(p_{irf}^{di} * f)_k = \sum_{j=1}^k (p_{irf}^{di})_j f_{k-j+1}. \quad (11)$$

The convergence of the summation in equation 11 is highly affected by the form of p_{irf}^{di} . (recall that, p_{irf}^{di} goes to infinity as $\tau \rightarrow 0$). As a result, the finer time sampling of p_{irf}^{di} (smaller $d\tau$) is not only required to correctly describe its values at the starting diffraction times (as discussed in previous paragraph), but also to yield converged/accurate results when convolved with the incident signal f (see equation 11). On the other hand, large numbers of time samples lead to dramatic increase of the computational speed. Therefore, a possible

reformulation of equation 10, in which p_{irf}^{di} is replaced by a non-singular and continuous function can provide convergent results for coarser time sampling and smaller calculation time.

In section 3 a set of such functions is introduced. The performance of these functions in the diffracted signal calculation can be further improved with the derivation of their corresponding generator curves, as it will be demonstrated in section 4.

2. Generator Curve Method

2.1. Theory

As demonstrated in previous work of the authors [8] the information of the impulse response for every source-receiver configuration and all diffraction times can be contained into a single curve, namely, *the generator curve*, $E^{i,r}(\Pi^{i,r})$,

$$E^{i,r}(\Pi^{i,r}) = \frac{4\sqrt{2}}{\pi\sqrt{\pi}\sqrt{\Pi^{i,r}}(\Pi^{i,r}+1)}, \quad (12)$$

(shown in Figure 2), where the parameters Π^i (associated with the incident signal) and Π^r (associated with the reflected signal) are dimensionless, termed *diffraction numbers*, and defined as

$$\Pi^i = \frac{\tau}{\tau_{lag}^i}, \quad \Pi^r = \frac{\tau}{\tau_{lag}^r}, \quad (13)$$

while the *scaled edge sources* E^i and E^r are also positive dimensionless quantities related to $p_{irf}^{di,dr}$ as follows,

$$p_{irf}^{di,dr} = -\frac{1}{4\pi} A_t \frac{\text{sign}(\Phi_{1,2})}{\sqrt{t_d t_1} \Phi_{1,2}^2} E^{i,r}. \quad (14)$$

The scaled edge sources $E^{i,r}$ express the product ($I \cdot d^{i,r}$), representing radiation from a directive line source, scaled by $\text{sign}(\Phi_{1,2})\sqrt{t_d t_1} \Phi_{1,2}^2$. The diffraction numbers $\Pi^{i,r}$ express the diffraction time τ normalized by the diffraction delay $\tau_{lag}^{i,r}$ (equation 9) and they can be thought of as universal parameters of diffraction. They represent diffraction time so normalized as to be independent of the source-receiver configuration (that is of the source-receiver location and also of the type of the incident signal). As demonstrated in ref. [8], the generator curve embodies/generates (i) all diffracted signals produced for any source-

receiver configuration, and (ii) the diffracted field around the half plane produced by any source at any diffraction time. For example, a random time τ corresponds to one value of Π^i (see equation 13) and thus to one value of E^i , (equation 12) which when multiplied by the factor $-\frac{1}{4\pi} A_t \frac{\text{sign}(\Phi_1)}{\sqrt{t_d t_1} \Phi_1^2}$ (equation 14) yields the value of p_{irf}^{di} .

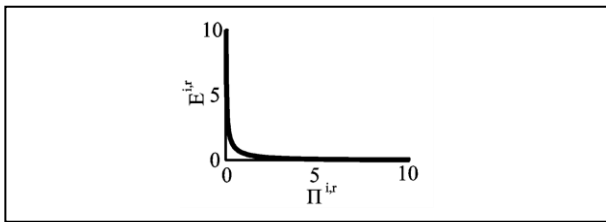


Figure 2. Generator curve $E^{i,r}(\Pi^{i,r})$ (equation 12) of the impulse response solution $p_{irf}^{di,dr}$.

In numerical calculations, which involve multiple source-receiver configurations, predicting the impulse response using the generator curve (equations 12-14) should provide significant computational advantage compared to direct computation (equations 2-5) of p_{irf}^d , as the generator curve is only computed once, while direct computation must be performed separately for each source-receiver configuration.

2.2 Computational results

In the following, it is demonstrated that the impulse response, p_{irf}^d , can be predicted by the generator curve method (equations 12-14) at a fraction of computational cost involved in direct computations (equations 2-5). For the purposes of comparison, an example of practical interest is considered.

Figure 3 shows an example of a traffic noise barrier shielding a city block. The barrier installation leaves the entire city block in the shadow region (see Figure 3b). The diffracted signal is calculated on a receiver grid of size $G \times G$, which lies on a plane perpendicular to the y -axis, just in front of the city block (see Figure 3b).

Figure 4 shows the achieved reduction of the CPU time when the generator curve (equations 12-14) is used instead of direct computation of p_{irf}^d (equations 2-5). The impulse response is computed for two different numbers of time samples

$M = 1000$ (Figure 4a) and $M = 2000$ (Figure 4b) on a grid of receiver locations shown in Figure 3. The reduction of the CPU time provided by generator curve method appears to increase, as the number of time samples and the grid size is increased. All calculations have been performed with MATLAB on a personal computer with Intel core i7-4710HQ at 2.50 GHz.

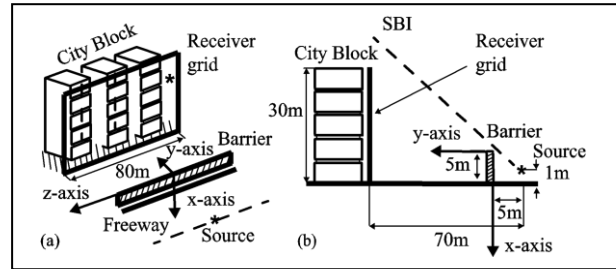


Figure 3. Geometry of a traffic noise barrier shielding a city block; perspective view (a), side view (b).

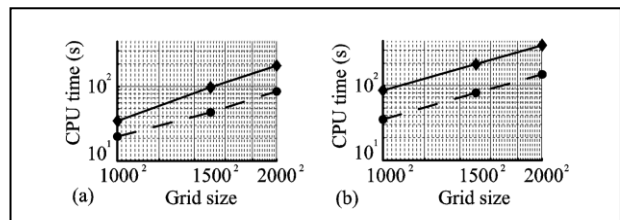


Figure 4. CPU time required to calculate the impulse response, p_{irf}^d , versus the receiver grid size $G \times G$ (receivers and source as shown in Figure 3), by direct computations (equations 2-5) (solid line) and by the generator curve method (equations 12-14) (dashed line) for $M = 1000$ timesamples (a), and $M = 2000$ time samples (b).

3. Antiderivatives method

In the previous section it was shown that the computation of the impulse response p_{irf}^d can be accelerated using the generator curve. The computation of the diffracted pulse p^d (equation 10) however, remains costly as the extra small time step $d\tau$ required to handle the initial points of p_{irf}^d ($p_{irf}^d \rightarrow \infty$ as $\tau \rightarrow 0$) affects dramatically the computational speed of digital convolution (equation 11). In this section, p_{irf}^d (used to compute equation 10) will be replaced with another non-singular and continuous function that will allow accurate convolution calculations at coarser time sampling.

3.1 Theory

A set of useful functions that can replace p_{irf}^d in the convolution process (equation 10) is introduced. The analysis is shown only for p_{irf}^d associated with the incident signal (see equations 4 and 5), but it is similar for p_{irf}^{dr} associated with the reflected signal.

Consider a set of functions a_n^{di} , $n=1,2,\dots$ such that p_{irf}^{di} is the n -th order partial time derivative of a_n^{di} ,

$$\frac{\partial^n a_n^{di}}{\partial \tau^n} = p_{irf}^{di}. \quad (15)$$

The function a_n^{di} is called n -th order partial time antiderivative of p_{irf}^{di} . An advantage of the specific analytical solution p_{irf}^{di} employed here is that its antiderivatives a_n^{di} exist for every physical number n and can be expressed in a closed form. Specifically, for the first three orders,

$$\begin{aligned} a_1^{di} &= c_{us}^i \arctan\left(\sqrt{\frac{\tau}{\tau_{lag}^i}}\right) \\ a_2^{di} &= c_{us}^i \tau_{lag}^i \left[\left(\frac{\tau}{\tau_{lag}^i} + 1\right) \arctan\left(\sqrt{\frac{\tau}{\tau_{lag}^i}}\right) - \sqrt{\frac{\tau}{\tau_{lag}^i}} \right], \quad (16) \\ a_3^{di} &= \frac{1}{2} c_{us}^i (\tau_{lag}^i)^2 \left[\left(\frac{\tau}{\tau_{lag}^i} + 1\right)^2 \arctan\left(\sqrt{\frac{\tau}{\tau_{lag}^i}}\right) \right. \\ &\quad \left. - \frac{1}{2} c_{us}^i (\tau_{lag}^i)^2 \sqrt{\frac{\tau}{\tau_{lag}^i}} \left[1 + \frac{5}{3} \left(\frac{\tau}{\tau_{lag}^i}\right) \right] \right] \end{aligned}$$

where $c_{us}^{i,r} = -A_s \sqrt{t_d^{-1} t_{1,2}} \Phi_{1,2} / (\pi \sqrt{\tau_{lag}^{i,r}})$.

Using the differentiation property of the convolution it can be proven that, instead of the impulse response, its antiderivatives can be used to compute the convolution

$$p^{di} = p_{irf}^{di} * f = \frac{\partial a_1^{di}}{\partial \tau} * f = a_1^{di} * \frac{\partial f}{\partial \tau}, \quad (17)$$

which can be generalized into,

$$p^{di} = a_n^{di} * \frac{\partial^n f}{\partial \tau^n}. \quad (18)$$

For convenience when referring to equation 18,

we will denote $p_{irf}^{di} \equiv a_0^{di}$ and $\frac{\partial^0 f}{\partial \tau^0} \equiv f$.

Figure 5 shows the antiderivatives up to order $n=3$ convolved with the corresponding n -th order time derivative of the incident signal (a one-period sinusoidal pulse).

The main difference between the impulse response (a_0^{di}) and its antiderivatives a_n^{di} , $n=1,2,\dots$ is the limiting behavior close to zero. The former goes to infinity [$a_0^{di}(0) \rightarrow \infty$], while the latter are continuous and bounded at zero [$a_n^{di}(0) = 0, n=1,2,\dots$]. As a result, in numerical calculations the traditional employment of the impulse response for the convolution requires very small time interval ($d\tau$) to accurately compute the values around $\tau=0$ and to produce convergent results, while employment of antiderivatives requires much coarser time sampling, which is translated to significant computational advantage, as it will be discussed in detail in the next section.

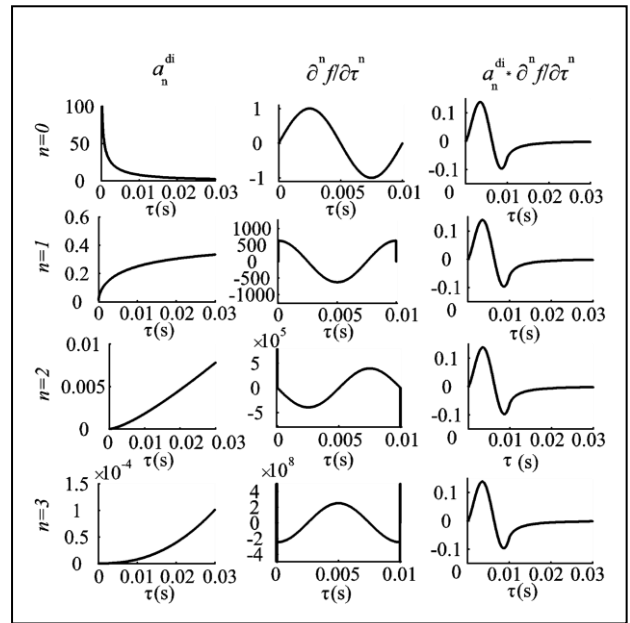


Figure 5. The diffracted pulse p^{di} (right column) predicted by equation 18 as convolution of a_n^{di} (left column) with $\frac{\partial^n f}{\partial \tau^n}$ (middle column) for several orders n ;

incident signal $f = \sin(2\pi\tau/T_{inc})$, $0 \leq \tau \leq T_{inc} = 0.01s$; source at $(r_0, \varphi_0, z_0) = (2cT_{inc}, \pi/2, 0)$; receiver at $(r, \varphi, z) = (cT_{inc}, \pi + \pi/2 + \pi/20, 0)$.

3.2 Computational results

In the previous section it was shown how a diffracted pulse can be calculated using any order n of equation 18. In this section it is examined, firstly, for which order n this result converges to an accurate prediction, as the number of time samples increases. Secondly, how much computational time is required to complete a p^{di} prediction using the n -th order of equation 18 for a certain level of accuracy. Specifically, it will be

shown that: (i) orders $n \geq 3$ should not be employed due to numerical oscillations introduced in the computation of the time derivatives as $d\tau \rightarrow 0$, (ii) orders $n=1, n=2$ require much fewer time samples than $n=0$ to achieve the same level of accuracy, and (iii) employment of orders $n=1, n=2$ reduces the CPU time by orders of magnitude compared to the traditional employment of the impulse response function ($n=0$) for the same level of accuracy.

A numerical example is depicted in Figure 6 with incident signal a one-period sinusoidal pulse $f = \sin(2\pi\tau/T_{inc})$, $0 \leq \tau \leq T_{inc} = 0.01s$. The diffracted pulse p^{di} is calculated by equation 18 up to order $n=3$. For each order, several sampling time steps $d\tau$ are used, spanning from $d\tau = 10^{-4}s$ (coarser sampling) to $d\tau = 10^{-8}s$ (finer sampling). The order $n=0$ (impulse response prediction) is expected to yield the correct result as $d\tau \rightarrow 0$. Thus, as benchmark prediction of p^{di} , we use an impulse response prediction $(p^{di})_{d\tau_0} = (p^{di}_{if} * f)_{d\tau_0}$ measured on an extra fine time array, having $d\tau_0$, so that $d\tau \gg d\tau_0$ for every $d\tau$. Then the error of convergence for each order n is defined as the maximum relative difference between the diffracted signal predicted by equation 18 with $d\tau$ and the benchmark prediction,

$$err_{d\tau}^n = \max \left(\frac{\left| \left(a_n^{di} * \frac{\partial^n f}{\partial \tau^n} \right)_{d\tau} - (p_{if}^{di} * f)_{d\tau_0} \right|}{\left| (p_{if}^{di} * f)_{d\tau_0} \right|} \right). \quad (19)$$

It is emphasized that, $err_{d\tau}^n$ is not only a measure of convergence but also, a measure of accuracy since, the extra fine $(p_{if}^{di} * f)_{d\tau_0}$ yields the correct values to predict p^{di} .

Figure 6 shows $err_{d\tau}^n$ versus the sampling time step $d\tau$, for each order of $a_n^{di} * \frac{\partial^n f}{\partial \tau^n}$ up to $n=3$.

As $d\tau \rightarrow 0$, the prediction $a_n^{di} * \frac{\partial^n f}{\partial \tau^n}$, appears to converge to accurate values ($err_{d\tau}^n \rightarrow 0$) for all depicted orders except $n=3$. The latter is attributed to the derivative term $\frac{\partial^n f}{\partial \tau^n}$, as it has been observed that the numerical differentiation produces oscillations for orders higher than $n=3$ when $d\tau \rightarrow 0$. From the orders n that do converge to accurate values ($n=0,1,2$), the impulse response prediction ($n=0$) requires a much finer

time sampling to achieve a level of error $err_{d\tau}^n$, while the orders $n=1$ and $n=2$ can reach the same level $err_{d\tau}^n$ using much fewer time samples. This phenomenon is, as discussed in the introduction (section 1.2), a result of the high resolution, that is required in the discretization of p_{if}^{di} to describe its starting times, where p_{if}^{di} goes to infinity. Finally, as the $n=2$ order converges faster to very small $err_{d\tau}^n$ it is the recommended choice for the diffracted pulse prediction.

In practical applications the diffracted signal will be calculated at several locations around the barrier and the convolution operation will be performed multiple times. Thus it is essential to provide an estimation of the CPU cost of the application of each method for specific accuracy.

Figure 7 presents an example of CPU time performance of the $n=0,1,2$ orders of equation 18 in predicting the entire diffracted signal ($p^d = p^{di} + p^{dr}$) on a receiver grid (shown in Figure 3) of size 50×50 , for accuracy $err_{d\tau}^n = 2\%$. As expected the orders $n=1$ and $n=2$ improve the computation speed of the impulse response prediction by an order of magnitude, with the $n=2$ order requiring the less CPU time to compute. Calculations have been performed with MATLAB on a personal computer with Intel core i7-4710HQ 2.50GHz processor.

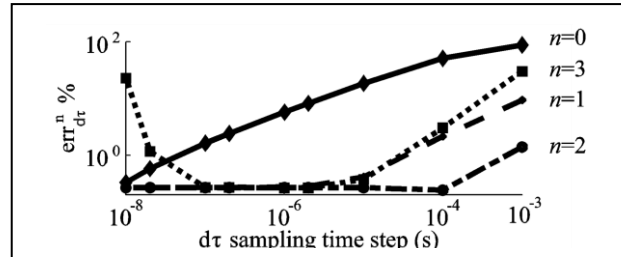


Figure 6. Error $err_{d\tau}^n$ (equation 19) versus sampling time step $d\tau$ of equation 18 up to order $n=3$; incident signal $f = \sin(2\pi\tau/T_{inc})$, $0 \leq \tau \leq T_{inc} = 0.01s$; source at $(r_0, \varphi_0, z_0) = (2cT_{inc}, \pi/2, 0)$; receiver at $(r, \varphi, z) = (cT_{inc}, \pi + \pi/2, 0)$.

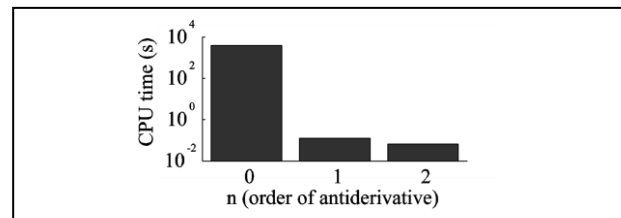


Figure 7. CPU time required to calculate the diffracted signal p^d with accuracy $err_{d\tau}^n = 2\%$ on a receiver grid of size 50×50 (receivers and source as shown in Figure 3) for several orders n of equation 18; incident signal $f = \sin(2\pi\tau/T_{inc})$, $0 \leq \tau \leq T_{inc} = 0.01s$;

4. Generator curve method for the antiderivatives

In the present section, the theory of the generator curve is extended to the antiderivatives of the impulse response (described in section 3) in order to further enhance their computational performance.

4.1. Theory

For the n -th ($n=1,2,\dots$) order antiderivative two quantities are defined as *scaled antiderivatives* g_n^i and g_n^r of the n -th order,

$$\begin{aligned} g_n^i &= \left[c_{us}^i (\tau_{lag}^i)^{n-1} \right]^{-1} a_n^{di} \\ g_n^r &= \left[c_{us}^r (\tau_{lag}^r)^{n-1} \right]^{-1} a_n^{dr} \end{aligned} \quad (20)$$

It can be proven that, g_n^i and g_n^r can be expressed as single-variable functions of the diffraction numbers Π^i and Π^r , respectively. Specifically, for the first three orders,

$$\begin{aligned} g_1^{i,r} &= \arctan(\sqrt{\Pi^{i,r}}) \\ g_2^{i,r} &= (\Pi^{i,r} + 1) \arctan(\sqrt{\Pi^{i,r}}) - \sqrt{\Pi^{i,r}} \\ g_3^{i,r} &= \frac{1}{2} (\Pi^{i,r} + 1)^2 \arctan(\sqrt{\Pi^{i,r}}) \\ &\quad - \frac{1}{2} \sqrt{\Pi^{i,r}} - \frac{5}{6} \sqrt{\Pi^{i,r}} \Pi^{i,r} \end{aligned} \quad (21)$$

Just as the scaled edge sources $E^i(\Pi^i)$ and $E^r(\Pi^r)$, the scaled antiderivatives for each order n are described by a single-variable function that forms the corresponding generator curve.

Figure 8 depicts the generator curves for the orders $n=1$ and $n=2$. $E^{i,r}(\Pi^{i,r})$ can be considered a generator curve $g_0^{i,r}$ of order $n=0$.

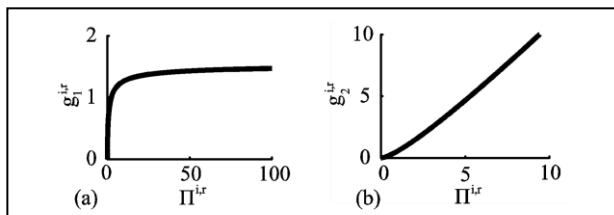


Figure 8. Generator curve $g_n^{i,r}$ (equation 21) of the antiderivatives of order $n=1$ (a) and $n=2$ (b).

The generator curve can be used, as described in section 2 for the impulse response, to predict the antiderivatives a_n^{di} and a_n^{dr} for any source-receiver configuration at any diffraction time τ by specifying its corresponding Π^i and Π^r (equation 13) from the generator curve and scaling the corresponding g_n^i and g_n^r as,

$$\begin{aligned} a_n^{di} &= \left[c_{us}^i (\tau_{lag}^i)^{n-1} \right] g_n^i \\ a_n^{dr} &= \left[c_{us}^r (\tau_{lag}^r)^{n-1} \right] g_n^r \end{aligned} \quad (22)$$

As opposed to direct computations of a_n^{di} and a_n^{dr} , the generator curve, $g_n^{i,r}(\Pi^{i,r})$, is only calculated once and thus it is expected to reduce the time of calculations.

4.2 Computational results

In the following the generator curves for the partial antiderivatives of orders $n=1$ and $n=2$ will be used to further accelerate the prediction of the diffracted signal. The presented comparisons regard the noise barrier-city block geometry shown in Figure 3. The diffracted signal is measured on a grid of receiver locations. In direct computations, a_n^{di} and a_n^{dr} are calculated at all diffraction times are then convolved with their corresponding time derivative of the incident signal. On the other hand, the generator curve is only computed once, its values g_n^i and g_n^r are assigned to the proper τ for every receiver (equation 13), scaled according to equation 22, and then convolved with the corresponding time derivative of the incident signal.

Figure 9 shows CPU time (required to calculate the diffracted signal p^d) comparisons between direct (equation 16) and generator curve (equation 21) computations for the antiderivatives of order $n=1$ and $n=2$, both for accuracy $err_{dr}^n = 2\%$. Two grids have been simulated one of size 1000x1000 (see Figure 9a) and another of size 1500x1500 (see Figure 9b). As expected the generator curve method is faster in all cases. It is also observed that the CPU time reduction increases as the grid size increases.

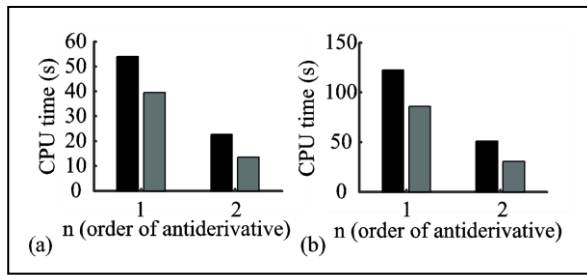


Figure 9. CPU time required to calculate the diffracted signal p^d with $err_{dr}^n = 2\%$ accuracy by direct computations (equations 16, 18) (black color) and by the generator curve method (equations 13, 18, 21, 22) (grey color) on a receiver grid (receivers and source as shown in Figure 3) of size 1000x1000 (a) and 1500x1500 (b); incident signal $f = \sin(2\pi\tau/T_{inc})$, $0 \leq \tau \leq T_{inc} = 0.01s$.

5. Conclusions

The present work focuses on reducing the computational cost required to produce accurate diffracted signal predictions. The analysis starts from an impulse response solution derived in previous work of the authors. The impulse response goes to infinity at its starting times. As a result, in numerical calculations, the impulse response requires dense time sampling not only to accurately describe its starting behavior but also, to yield convergent results when convolved with the incident signal to predict the diffracted signal. The later requirement affects the computational speed dramatically, especially for cases involving multiple receivers, considering that the digital convolution is computed as a summation for every time sample.

To deal with these issues, the authors have presented two new methods in predicting the diffracted signal. The first is the generator curve method. The generator curve $E^{i,r}(\Pi^{i,r})$ embodies/generates all impulse response functions at all diffraction times. The generator curve method has been found to accelerate the impulse response calculation, as $E^{i,r}(\Pi^{i,r})$ is computed once and then its values are stretched and scaled to produce the impulse response for any source-receiver configuration.

The second method is based on the impulse response time partial antiderivatives $a_n^{di,dr}$. The antiderivatives as opposed to the impulse response are continuous and non-singular functions, which when convolved with the corresponding time

derivative $\frac{\partial^n f}{\partial \tau^n}$ of the incident signal f can predict the diffracted signal. The performance of the antiderivatives of several orders has been tested with numerical examples. The orders $n=1$ and $n=2$ have been found to produce convergent results with much lesser times samples than those required for the impulse response. As a result the $n=1$ and $n=2$ antiderivatives can reduce the computation speed of the diffracted signal by an order of magnitude, with $n=2$ being faster than $n=1$ in the presented examples.

The performance of the antiderivatives method has been further improved with the introduction of the antiderivatives generator curves $g^{i,r}(\Pi^{i,r})$. Just as the generator curve of the impulse response, $g^{i,r}$ generates $a_n^{di,dr}$ at any source-receiver configuration and any diffraction time. Thus, in cases involving multiple receivers it is only computed once and its values are stretched and scaled to produce a faster result compared to direct computations of $a_n^{di,dr}$.

References

- [1] K. M. Li, H. Y. Wong: A review of commonly used analytical and empirical formulae for predicting sound diffracted by a thin screen. Appl. Acoust. 66 (2005) 45–76.
- [2] M. Baulac, J. Defrance, P. Jean, and F. Minard: Efficiency of noise protections in urban areas: Predictions and scale model measurements. Acta Acustica united with Acustica 92 (2006) 530–539.
- [3] U. M. Stephenson: Quantized pyramidal beam tracing - a new algorithm for room acoustics and noise immission prognosis. Acta Acustica 82 (1996) 517–525.
- [4] F. G. Friedlander: On the half plane diffraction problem. Quar. J. Mech. Appl. Math. 4 (1951) 344–357.
- [5] D. Ouis: Diffraction by a hard half-plane: Useful approximations to an exact formulation. J. Sound Vib. 252 (2002) 191–221.
- [6] J. P. Chambers and Y. H. Berthelot: Time-domain experiments on the diffraction of sound by a step discontinuity. J. Acoust. Soc. Am. 96 (1994) 1887–1892.
- [7] S. Sakamoto, T. Seimiya, and H. Tachibana: Visualization of sound reflection and diffraction using finite difference time domain method. Acoust. Sci. Technol. 23 (2002) 34–39.
- [8] P. Menounou and P. Nikolaou: Analytical model for predicting edge diffraction in the time domain. J. Acoust. Soc. Am. 142 (2017) 3580–3592.